ARTICLE

Flexible Planar Micro-supercapacitors Based on Carbon Nanotubes

Wen-xiang Cheng, Tong-tong Jiang*, Hai-bo Hu

School of Physics and Materials Science, Key Laboratory of Structure and Functional Regulation of Hybrid Materials, Anhui University, Hefei 230039, China

(Dated: Received on August 24, 2020; Accepted on September 15, 2020)

The boom in ultra-thin electronic devices and the growing need for humanization greatly facilitated the development of wearable flexible micro-devices. But the technology to deposit electrode material on flexible substrate is still in its infancy. Herein, the flexible symmetric micro-supercapacitors made of carbon nanotubes (CNTs) on commercial printing paper as electrode materials were fabricated by combining tetrahedral preparator auxiliary coating method and laser-cutting interdigital configuration technique on a large scale. The electrochemical performance of the obtained micro-supercapacitors can be controlled and tuned by simple choosing the different models of tetrahedral preparatory to obtain CNTs film of different thicknesses. As expected, the micro-supercapacitor based on CNTs film can deliver an areal capacitance of up to 4.56 mF/cm^2 at current of 0.02 mA. Even if, micro-supercapacitor undergoes continuous 10000 cycles, the performance of device can still remain nearly 100%. The as-demonstrated tetrahedral preparator auxiliary coating method and laser-cutting interdigital configuration technique provide new perspective for preparing microelectronics in an economical way. The paper electrode appended by CNTs achieves steerable areal capacitance, showing broad application prospect in fabricating asymmetric micro-supercapacitor with flexible planar configurations in the future.

Key words: Carbon nanotubes, Supercapacitors, Flexible planar configurations

I. INTRODUCTION

With the rapid boom of portable electronic devices, wireless sensor networks and increasingly serious problem of environment population caused by traditional energy excessive consumption, delicate and flexible new energy source (such as photovoltaic cells, supercapacitors) starts to come into people' view [1−5]. In terms of charging property, cells are typically charged with a certain voltage, limited lifetime and low power density [6, 7]. While supercapacitor can be charged with maximum current and can be powered by supplier with lower cost, higher cycling and power density than these of batteries [8−10]. Therefore, micro-supercapacitors have become new-emerging energy storage for offering a superior frequency response and excellent rate capability [11, 12]. Miniaturizing energy storage devices is beneficial for them to be integrated directly with the chips and facilitate the fabrication of complex equipment with multiple functions. In addition, planarization of microdevices can simplify the complexity of circuit design in the process of integrating discrete power sources into microelectromechanical systems [13, 14]. In terms of miniaturization and planarization, electrochemical micro-supercapacitors with two-dimensional configuration have attracted a lot of attention. The basic configuration of electrode contains substrate, electrode materials film and current collectors, which would influence the performance of micro-supercapacitors. The assembly of elementary composition for micro-supercapacitors greatly depends on the fabrication technology.

According to previous reports, the electrode in all-solid-state flexible ultrathin micro-supercapacitors can be fabricated by combining photolithography with electrophoresis technology [2] or using a vacuum filtration process followed by transferring thin film to polyethylene terephthalate (PET) as the working electrodes [15]. These fabrication processes involved complex steps, which is not beneficial for fabricating planar configurations of flexible supercapacitors on a large scale. In addition, generally, Au film usually need be used as current collectors, which greatly increase the cost of preparation. From a business point of view, it is highly necessary to develop a facile assembly technology, which can decrease the cost and maximize the capacitive performance of electrode materials at the same time. The first thing for exploring fabrication techniques is to determine the substrate, electrode materials film and current collectors.

Paper is an unconventional substrate with low cost. The cellulose fibers of paper with hierarchical arrangement and high solution absorption provide porous and

*Author to whom correspondence should be addressed. E-mail: jtt@ahu.edu.cn

DOI:10.1063/1674-0068/cjcp2008149

rough surface for efficient adhesion of active materials [16, 17]. Therefore, paper can be used as an ideal flexible substrate.

On the basis of energy storage mechanism, supercapacitor can be divided into two categories, including pseudo-capacitors and electrical double-layer capacitors (EDLCs) [18−20]. Pseudo-capacitors storing energy depend on faradic reactions at the surface of the electrode materials. The typical pseudo-capacitance materials are metal oxides, which usually show poor electrical conductivity. EDLCs store energy by adsorbing electrolyte ions on the surface of electrode. Carbon based nanomaterials, such as carbon sphere, carbon nanotube (CNT), are usually used as the electrode materials of EDLCs [21−23]. Among them, CNTs have attracted much attention due to their freestanding, flexible skeleton and conductive network structures [24]. CNTs not only can be used as electrode active materials of flexible electronic devices, but also can act as current collectors due to their excellent electrical conductivity, avoiding the complex process of depositing current collector materials [24, 25]. CNT can be endowed with strong adhesion by introducing oxygen functional groups to interact with electrodes [26]. In addition, CNTs also can integrate with other materials to further optimize the performance of supercapacitor [27]. Based on these merits, CNT film on paper is expected to be a desirable electrode for exploring the assembly technology, process and architecture of micro-supercapacitor device [28, 29].

In this work, tetrahedral preparator auxiliary coating method and direct laser machining process were used to fabricate interdigital electrode made of CNT film deposited on office printing paper. The obtained CNT flexible interdigital electrodes were assembled to fabricate planar micro-supercapacitors. The electrical performance of symmetric supercapacitors with three kinds of CNT interdigital electrodes prepared by tuning model parameter of tetrahedral preparator was measured. The results testify that the areal capacitance of as-prepared symmetric supercapacitor depends on the thickness of CNT film, which can be easily tailored. Combined with inherent advantages of paper, this work advances the commercialization process for micro-energy storage and conversion devices.

II. METHODS

A. Preparation of interdigital microelectrodes

In order to form a CNT ink, CNTs were dispersed in deionized water with a concentration of 200 mg/mL by ultra-sounding deposition for 30 min to obtain product A. In addition, sodium carboxymethyl cellulose (CMC) was dispersed in deionized water with a concentration of 20 mg/mL to obtain product B. And then, product B was added to product A to mix together for obtaining the ultimate ink. Next, the CNT ink was dipped on the surface of commercial printing paper followed by uniformly pulling the tetrahedral preparator with different standards to obtain CNT coated film.

B. Construction of symmetrical micro-supercapacitors

Polyvinyl alcohol (PVA) was added into purified water with stirring at the temperature of 90 °C for 2 h. Next, H_2SO_4 was added into the PVA solution under the disposition of stirring to obtain 1 mol/L H_2SO_4/PVA electrolyte. Interdigital CNT film coated paper electrode was moulded by laser beam cutting. The obtained interdigital electrode can be fixed to any substrate by double sided adhesive tape.

C. Electrochemical tests

Typically, the electrochemical performance of as-fabricated symmetrical micro-supercapacitors was conducted by employing three-electrode system using CHI760D (ChenHua/Shanghai) workstation. Electrochemistry impedance spectroscopy (EIS) curve was acquired by selecting frequency range of 0.01−100 kHz. Cyclic voltammetry (CV) and galvanostatic charge/discharge (GCD) curves were explored to investigate electrochemical quality under different scanning rates and currents, respectively.

III. RESULTS AND DISCUSSION

The detailed procedure for fabricating micro-supercapacitors is schematically presented in FIG. 1. First, CMC and CNT were added into deionized water to mix together with a ratio of 1:9 for preparing CNT ink sizing agent. Among them, CMC was used as adhesive for efficiently connecting CNT and facilitating the imbedding of ink sizing agent on paper matrix. Based on the intrinsic properties of printing paper such solvent absorbability and the stronger adhesion force with CNT ink sizing agent, tetrahedral preparator auxiliary coating method was adopted to coat CNT ink sizing agent on daily printing paper. With drying at 60 °C for 12 h, the CNT film was uniformly deposited covering the entire A4 printing paper. The uniformity coefficient of ink sizing agent and solvent evaporation kinetics process determine the flatness of CNT film. The designed profile of interdigital electrode was imported into the laser machining to control the movement of laser beam. The local high temperature of laser beam induced fusion of CNT/paper matrix in imported pattern to engrave symmetrical interdigital electrode. The obtained interdigital electrode can be transferred to PET or glass substrate by double faced adhesive tape. Next, H_2SO_4/PVA hydrogel electrolyte was deposited to the

DOI:10.1063/1674-0068/cjcp2008149

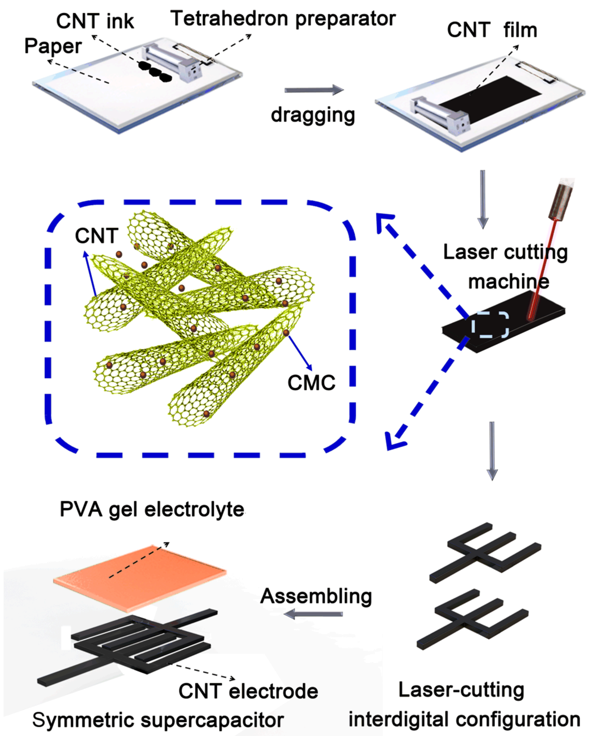

FIG. 1 Flow chart of fabricating symmetric micro-supercapacitors.

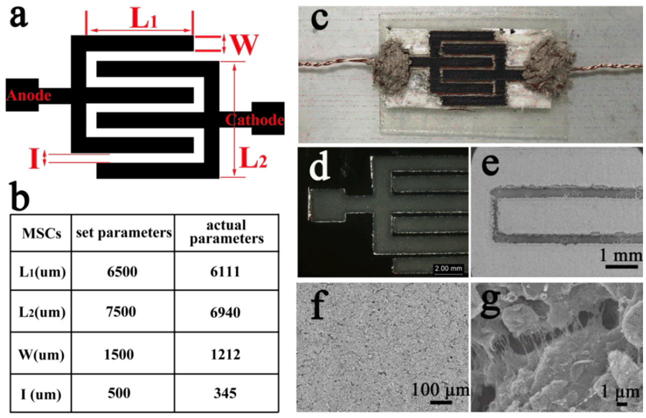

FIG. 2 (a) The designed shape construction of interdigital electrode. (b) The designed parameters and actual parameters of interdigital electrode. (c) The interdigital electrode real products. (d) Optical micro-image of interdigital electrode. (e) SEM image of interdigital electrode. (f) Low resolution SEM image of electrode material. (g) High resolution SEM image of electrode material.

electrode for realizing the assembling of symmetrical micro-supercapacitor.

FIG. 2(a) shows the designed electrode contour and shape parameters associated with the electrode. To calculate the precise area of the electrode, actual parameters of interdigital electrode were measured to compare with the designed parameters in laser cutting machine, as shown in FIG. 2(b). Obviously, the width of interdigital electrode and the space between two electrodes are consistent with the designed parameters in laser machining. The sum of actual length of interdigital electrode approaches 2.5 cm, while the width of that is 0.121 cm with interval of 0.345 mm. According to these parameters, the electrode area for whole device was calculated to be about 0.6 cm^2. Seen from real products, the optical micro-image and scanning electron microscope (SEM) of CNT/paper interdigital electrode, it can be found that the path area of laser beam is CNT material-free, indicating the efficient removement of material on pattern boundary by laser patterning technology, which availably avoid short circuit phenomenon. In addition, non-conducting substrate (paper/PET) can be selected as a supporting plane to prevent the contact between two electrodes. The interdigital electrode real products, optical micro-image and SEM image of interdigital electrode show that the edges of electrode are uniform (FIG. 2(c), (d) and (e)). Seen from low resolution SEM image of electrode material (FIG. 2(f)), it can be deduced that the CNT film is very smooth as a whole. When the SEM image of electrode material is enlarged, it can be found that there are enough CNTs even in the position of some small cracks (FIG. 2(g)), connecting each part of CNT film, which is conductive to providing faster electronic channel.

In order to demonstrate the cutting power of laser beam and further explore the influence of CNT film thickness on the performance of a supercapacitor, CNT films of different thicknesses were obtained by selecting different models of tetrahedral preparators for controlling the distance between drawing rod of tetrahedral preparators and A4 printing paper. As shown in FIG. 3(a, b c), through replacing and using different tetrahedral preparators, the three CNT films with thicknesses of about 100 μm, 120 μm and 140 μm were obtained, which were referred as CNT-1 film, CNT-2 film, CNT-3 film, respectively. The obtained structure of CNT electrode shows intricately linked CNT layer without apparent void layer judge by the intimate contact of CNT with paper, which was endowed by the coarse surface of paper and the adhesive attraction of CMC (FIG. 3 (d)). Seen from the SEM image (FIG. 3(e, f)), there are many micro-nano empties formed by tubular interlacing structure, which can act as storage to contain abundant aqueous electrolyte providing larger contact area between CNT electrode and electrolyte as well as enough ionic conduction channel for electrolyte ion of CNT micro-supercapacitors [30].

With the aim of exploring the electrochemical performance of CNT based micro-supercapacitors with symmetric configuration, CV curves were measured by employing H_2SO_4 and polyvinyl alcohol (PVA) gel as electrolyte in two-electrode configuration. FIG. 4(a, b, c) show CV curves of micro-supercapacitors fabricated with CNT-1, CNT-2, CNT-3 electrode at various scan

DOI:10.1063/1674-0068/cjcp2008149

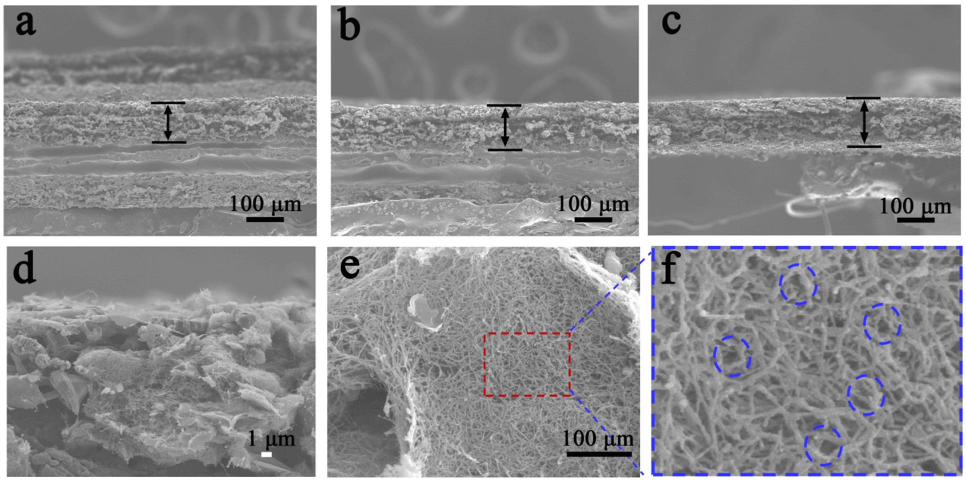

FIG. 3 SEM images of the samples obtained by choosing different models of tetrahedral preparators: Cross-section diagram of (a) CNT-1 electrode, (b) CNT-2 electrode. (c) CNT-3 electrode. (d) Magnified cross-section diagram of CNT-3 electrode. (e, f) Vertical view-image of CNT-3 film.

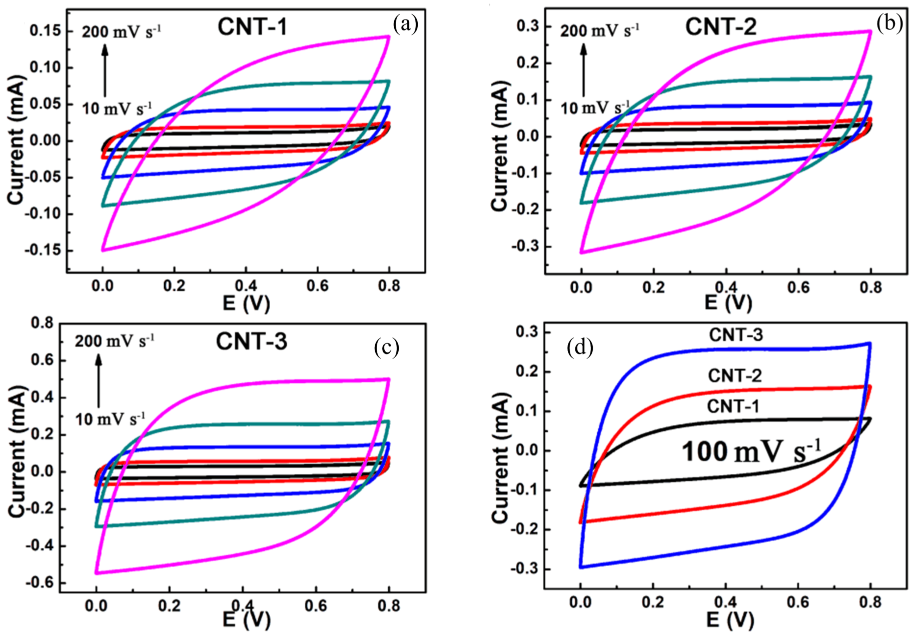

FIG. 4 CV curves at scan rates of 10, 20, 50, 100, and 200 mV/s of (a) CNT-1 micro-supercapacitor, (b) CNT-2 micro-supercapacitor, (c) CNT-3 micro-supercapacitor. (d) CV curve comparison of CNT-1, CNT-2, CNT-3 micro-supercapacitors at scan rates of 100 mV/s.

rates of 10, 20, 50, 100 and 200 mV/s, respectively. It can be deduced that the CNT micro-supercapacitors show voltage window from 0 V to 0.8 V. The CV curve presents rectangular shape, indicating electrochemical double layer capacitors behaviors. With the increase of scan rate, the integral area of CV curve for the three micro-supercapacitors gradually increases. In higher scan rates, CNT-3 micro-supercapacitor still maintains superior rectangular shape. But for CNT-1 and CNT-2 micro-supercapacitors, the shape of CV curve begins to deviate rectangular, indicating that the CNT-3 micro-supercapacitor exhibits the weaker resistive behavior endowed by efficient interlayer charge transfer as well as purer capacitive behavior even at high scan rates of 200 mV/s [12]. In addition, the integral area of CV curve for CNT-3 micro-supercapacitor is apparently larger than those of CNT-1 and CNT-2 (FIG. 4(d)), demonstrating the higher capacitance of CNT-3 micro-supercapacitor, which can be attributed to the larger thickness that provides larger interlayer spacing for insertion of the electrolyte ion and thus facilitating the enhancement for ionic conduction. The in-plane de-

DOI:10.1063/1674-0068/cjcp2008149

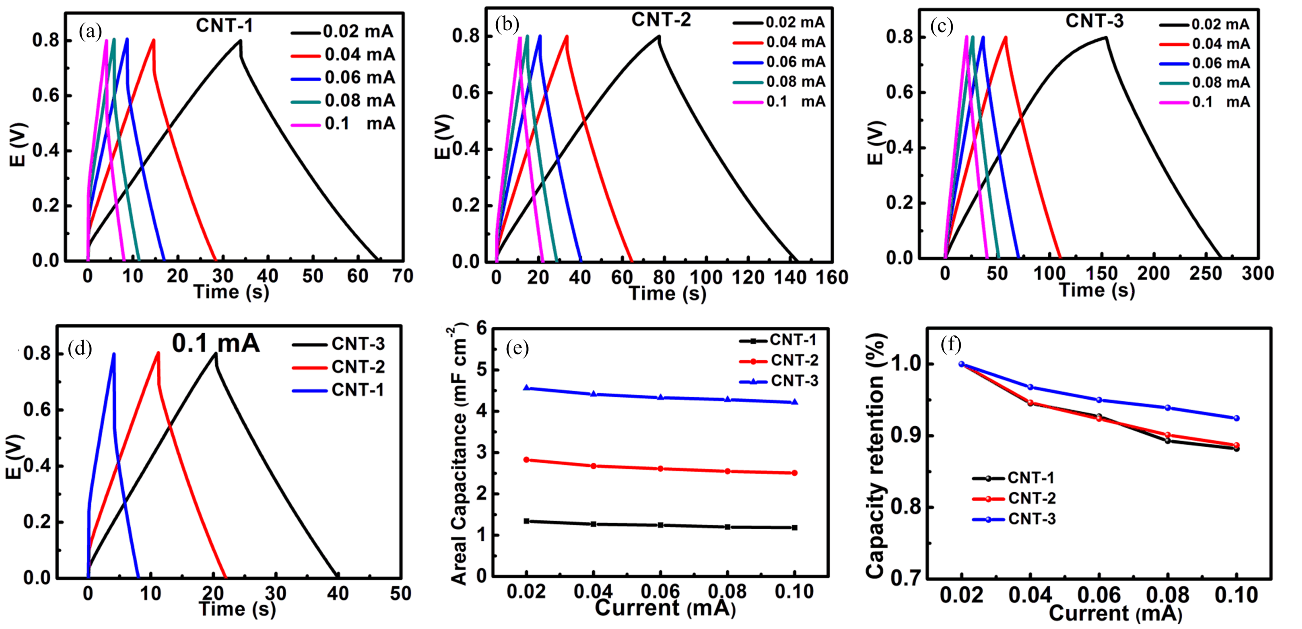

FIG. 5 GCD curves at various currents from 0.02 mA, 0.04 mA, 0.06 mA, 0.08 mA to 0.1 mA of (a) CNT-1, (b) CNT-2, (c) CNT-3 micro-supercapacitors. (d) GCD curves of CNT-1, CNT-2 and CNT-3 at current of 0.1 mA. (e) Areal capacitance of CNT-1, CNT-2, and CNT-3 under different currents. (f) Capacity retention of CNT-1, CNT-2, and CNT-3.

TABLE I Comparison of areal capacitance C of electrochemical double-layer micro-supercapacitors.

Electrode materials	Configuration	Electrolyte	C/(mF/cm^2)	Ref.
CNT	Interdigital	(PVA)/H_2SO_4 electrolyte (1 mol/L)	4.56	This work
Carbon/CNT(carbon)	Interdigital	(PVA)/H_2SO_4 electrolyte (1 mol/L)	4.80 (3.52)	[27]
Reduced graphite oxide[a]	In-plane circular	Graphite oxide serves as a solid electrolyte	0.51	[33]
Onion-like Carbon	Interdigital	Et_4NBF_4/anhydrous propylene carbonate[b]	0.9	[4]
Oxidized CNTs	Sandwich	Ionic-liquid-based electrolyte (PYR14TFSI)	~2.1	[26]

[a] With micrometre resolution.
[b] With concentration of 1 mol/L.

sign of interdigital CNT electrodes makes the CNT film electrode exhibit high accessible ionic conductance. In addition, compact side to side design of the electrodes (about 0.345 mm) shorts the distance between electrodes decreasing diffusion ions way. Compared with CNT-1, CNT-2 electrodes, the thicker film for CNT-3 electrodes possesses larger cross section facilitating the improvement of electro-chemical activity.

For the sake of further exploring the electrochemical performance of micro-supercapacitors, GCD tests were conducted to research the capacitive specialty of devices with potential windows between 0 and 0.8 V. The micro-supercapacitor fabricated with CNT interdigital electrodes possesses linear and symmetric GCD curve. By comparison, the IR drop of CNT-3 micro-supercapacitor is smaller than that of CNT-1, CNT-2, indicating the excellent electrical conductivity (FIG. 5(a, b, c)). The areal capacitance can be calculated judging by the relationship [31, 32]:

$$C=\frac{I}{(\mathrm{d}V/\mathrm{d}t)}S \tag{1}$$

where I represents the discharge current, $\mathrm{d}V/\mathrm{d}t$ represents the slope of the discharge curve, and S represents the total areal of the active electrode materials.

The interdigital CNT-3 micro-supercapacitor shows areal capacitance of 4.56, 4.41, 4.33, 4.28, 4.21 mF/cm^2 at different currents of 0.02, 0.04, 0.06, 0.08, and 0.1 mA, respectively. The areal capacitance of CNT-3 micro-supercapacitor is larger than those of CNT-1, CNT-2 micro-supercapacitors (FIG. 5(d)), and comparable to previously reported electrochemical double-layer micro-supercapacitors (Table I). In terms of the result of the charge/discharge curves, the almost isosceles triangle for the GCD curve of CNT micro-supercapacitors manifests their high coulombic efficiency, indicating the superior charge/discharge reversibility. Seen from FIG. 5(e), the areal capacitance

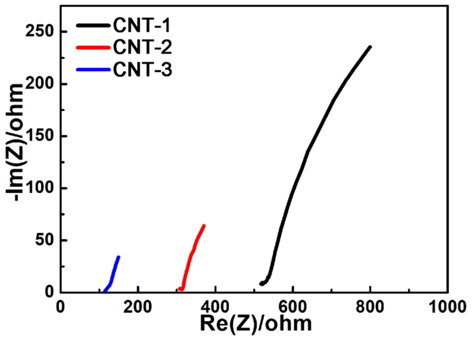

FIG. 6 EIS curves of CNT-1, CNT-2, and CNT-3 micro-supercapacitors.

of as-fabricated CNT-2 micro-supercapacitor is larger than that of CNT-1 micro-supercapacitor and lower than that of CNT-3 micro-supercapacitor, indicating that the areal capacitance of micro-supercapacitor fabricated with the developed method in this work depends on the thickness of CNT film. When the CNT film was used as one electrode of asymmetric micro-supercapacitor, the well-designed tetrahedral preparator auxiliary coating method and laser-cutting interdigital configuration technique are expected as new strategies for application in tuning the positive and negative electrode capacities match problem. At smaller density intensity, the specific capacitance presents large value, which can be attributed to the weak current which can guarantee plenty of time so that ions have enough charge-accumulation time to insure the interactions of ions with CNT materials [8]. When current of CNT micro-supercapacitors increases from 0.02 mA to 0.1 mA, areal capacitance still can retain 90% indicating enough efficient infiltration of ions into CNT film at higher scan rates (FIG. 5(f)).

The EIS measurement was used to investigate the feature of supercapacitors. Clearly, the obtained micro-supercapacitor has almost a straight line in the low frequency regions of Nyquist plots, showing typical EDLCs behavior (FIG. 6). The 45° Warburg region is related with diffusion of the electrolyte ions into CNT electrode [7]. The Warburg region of CNT-3 micro-supercapacitor is shorter, indicating their better diffusion of ions into the electrode. X-intercepts of Nyquist plots represent the equivalent series resistance (ESR). CNT-3 micro-supercapacitor shows lower ESR compared with CNT-1 and CNT-2 devices, which should be due to that CNT-3 device provides with large surface area in favor of transfer of electrolyte ions.

As a significant index of miniature device, the stability determines the application prospect of micro-devices in a sense. In the light of in-depth understanding micro-supercapacitors based on CNT film, the long-term durability measurement was conducted at a certain current density of 0.8 mA/cm^2 under cycling for 10000 cycles. As shown in FIG. 7, the relationship of capacity re-

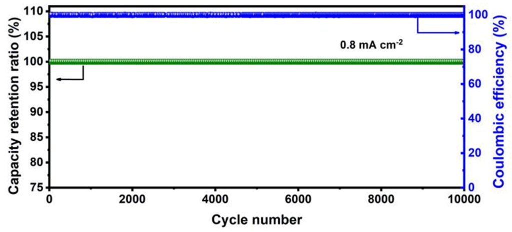

FIG. 7 Capacity retention and coulombic efficiency of CNT-3 micro-supercapacitor.

tention ratio, estimated coulombic efficiency and cycle number represents a horizontal line approaching 100%. The extremely stable capacitance can be attributed to intrinsic stability of CNT and the well-designed electrode configuration with short diffusion path. The economical film-forming technology and ingenious plane configuration design provide new perspective for commercial supercapacitors. The paper based interdigital electrode can expose the surface of paper to combine with double-sided tape for the sake of fixing electrode and also can be simply assembled realizing series/parallel of device.

IV. CONCLUSION

In summary, we have prepared interdigital electrode with CNT film by combining tetrahedral preparator auxiliary coating method and laser-cutting interdigital configuration technique. The obtained symmetrical micro-supercapacitors with CNT interdigital electrode show superior areal capacitance and long-terms durability. In addition, it was deduced that the areal capacitance of the obtained symmetrical micro-supercapacitors can be easily tuned by applying different models of tetrahedral preparators. Taking advantage of the low cost and easily tunable areal capacitance, the interdigital electrode made by CNT film shows bright prospect for fabricating micro-supercapacitor in the commercial applications of the future.

V. ACKNOWLEDGMENTS

This work was supported by the National Natural Science Foundation of China (No.51701002, No.51871001, and No.51672001)

[1] M. A. Bavioa, G. G. Acosta, T. Kessler, and A. Visintin, Energy **130**, 22 (2017).
[2] Z. Q. Niu, L. Zhang, L. L. Liu, B. Zhu, H. B. Dong, and X. D. Chen, Adv. Mater. **25**, 4035 (2013).
[3] J. Y. Song, S. Duan, X. Chen, X. J. Li, B. C. Yang, and X. B. Li, Chin. Phys. Lett. **37**, 076203 (2020).

DOI:10.1063/1674-0068/cjcp2008149

[4] K. Tang, C. Z. Yuan, Y. Xiong, H. B. Hu, and M. Z. Wu, Appl. Catal. B Environ. **260**, 118209 (2020).
[5] T. T. Jiang, H. B. Hu, F. C. Lei, J. J. Hu, M. Z. Wu, and D. Ho, ACS Appl. Mater. Interfaces **12**, 38031 (2020).
[6] D. Pech, M. Brunet, H. Durou, P. H. Huang, V. Mochalin, Y. Gogotsi, P. L. Taberna, and P. Simon, Nat. Nanotechnol. **5**, 651 (2010).
[7] B. Liu, B. Liu, Q. F. Wang, X. F. Wang, Q. Y. Xiang, D. Chen, and G. Z. Shen, ACS Appl. Mater. Interfaces **5**, 10011 (2013).
[8] B. Wang, J. Park, D. Su, C. Y. Wang, H. Ahn, and G. X. Wang, J. Mater. Chem. **22**, 15750 (2012).
[9] D. Y. Zhang, Y. H. Zhang, X. W. Li, Y. S. Luo, H. W. Huang, J. P. Wang, and P. K. Chu, J. Mater. Chem. A **4**, 568 (2016).
[10] Y. D. Wu, H. B. Hu, C. Z. Yuan, and M. Z. Wu, Nano Energy **74**, 104812 (2020).
[11] S. Q. Jiao, A. G. Zhou, M. Z. Wu, and H. B. Hu, Adv. Sci. **6**, 1900529 (2019).
[12] M. Beidaghi and C. L. Wang, Adv. Funct. Mater. **22**, 4501 (2012).
[13] H. B. Hu, Z. B. Pei, and C. H. Ye, Energy Storage Mater. **1**, 82 (2015).
[14] J. Lin, C. G. Zhang, Z. Yan, Y. Zhu, Z. W. Peng, R. H. Hauge, D. Natelson, and J. M. Tour, Nano Lett. **13**, 72 (2013).
[15] L. Peng, X. Peng, B. Liu, C. Z. Wu, Y. Xie, and G. H. Yu, Nano Lett. **13**, 2151 (2013).
[16] N. Kurra, B. Ahmed, Y. Gogotsi, and H. N. Alshareef, Adv. Energy Mater. 1601372 (2016).
[17] L. B. Hu, J. W. Choi, Y. Yang, S. Jeong, F. L. Mantia, L. F. Cui, and Y. Cui, Proc. Natl. Acad. Sci. USA **106**, 21490 (2009).
[18] C. C. Xiang, M. Li, M. J. Zhi, A. Manivannan, and N. Q. Wu, J. Power Sources **226**, 65 (2013).
[19] S. Sahoo and J. J. Shim, ACS Sustainable Chem. Eng. **5**, 241 (2017).
[20] S. Abouali, M. A. Garakani, B. Zhang, Z. L. Xu, E. K. Heidari, J. Q. Huang, J. Q. Huang, and J. K. Kim, ACS Appl. Mater. Interfaces **7**, 13503 (2015).
[21] A. K. Singh, D. Sarkar, K. Karmakar, K. Mandal, and G. G. Khan, ACS Appl. Mater. Interfaces **8**, 20786 (2016).
[22] M. Kaempgen, C. K. Chan, J. Ma, Y. Cui, and G. Gruner, Nano Lett. **9**, 1872 (2009).
[23] E. Frackowiak, V. Khomenko, K. Jurewicz, K. Lota, F. Béguin, J. Power Sources **153**, 413 (2006).
[24] Y. J. Zheng, Z. Q. Lin, W. J. Chen, B. H. Liang, H. W. Du, R. L. Yang, X. F. He, Z. K. Tang, and X. C. Gui, J. Mater. Chem. A **5**, 5886 (2017).
[25] C. Choi, J. A. Lee, A. Y. Choi, Y. T. Kim, X. Lepr´, M. D. Lima, R. H. Baughman, and S. J. Kim, Adv. Mater. **26**, 2059 (2014).
[26] M. G. Kim, B. Y. Lee, M. C. Li, S. Noda, C. S. Kim, J. Kim, W. J. Song, S. W. Lee, and O. Brand, ACS Nano **14**, 5659 (2020).
[27] L. He, T. J. Hong, Y. Huang, B. Xiong, X. F. Hong, M. Tahir, W. A. Haider, and Y. L. Han, Micromachines **10**, 307 (2019).
[28] Y. Pan, H. Gao, M. Y. Zhang, L. Li, G. N. Wang, and X. Y. Shan, J. Colloid Interface Sci. **497**, 50 (2017).
[29] J. X. Zhao, C. W. Li, Q. C. Zhang, J. Zhang, X. N. Wang, Z. Y. Lin, J. J. Wang, W. B. Lv, C. H. Lu, C. P. Wong, and Y. G. Yao, J. Mater. Chem. A **5**, 6928 (2017).
[30] D. Ghosh, J. Lim, R. Narayan, and S. O. Kim, ACS Appl. Mater. Interfaces **8**, 22253 (2016).
[31] Q. H. Wang, Y. X. Zhu, J. Xue, X. S. Zhao, Z. P. Guo, and C. Wang, ACS Appl. Mater. Interfaces **8**, 17226 (2016).
[32] L. Huang, D. C. Chen, Y. Ding, S. Feng, Z. L. Wang, and M. L. Liu, Nano Lett. **13**, 3135 (2013).
[33] W. Gao, N. Singh, L. Song, Z. Liu, A. L. M. Reddy, L. J. Ci, R. Vajtai, Q. Zhang, B. Q. Wei, and P. M. Ajayan, Nat. Nanotechnol. **6**, 496 (2011).

DOI:10.1063/1674-0068/cjcp2008149